

Supporting material

Direct Detection of α -Synuclein Dimerization Dynamics: Single-molecule Fluorescence Analysis

Zhengjian Lv[#], Alexey V. Krasnoslobodtsev[#], Yuliang Zhang[#], Daniel Ysselstein[‡], Jean-Christophe Rochet[‡], Scott Blanchard[¶] and Yuri L. Lyubchenko^{#*}.

Supporting materials and methods

α -Synuclein Proteins

Wild-type A140C α -synuclein in which the C-terminal alanine was replaced with a cysteine and the double mutants A30P-A140C, A53T-A140C and E46K-A140C were prepared as described in(1, 2). cDNAs encoding double cysteinyl α -Syn variant (V3C-A140C) was amplified by PCR and subcloned as Nde I – Hind III fragments into the vector pT7-7. The sequence of the α -Syn-encoding insert in each construct was verified using an Applied Biosystems (ABI 3730 XL) DNA sequencer. The double cysteinyl α -Syn variant was expressed in the E. coli strain BL21 (DE3) and purified as described(1, 2). Each α -Syn variant was further purified by reverse phase high performance liquid chromatography and analyzed by matrix assisted laser desorption ionization (MALDI) mass spectrometry. The mass-to-charge (m/z) values obtained from the MALDI analysis corresponded to the predicted values for full-length α -Syn.

Labeling of α -Syn with fluorophore

α -Syn solutions were freshly prepared by dissolving 0.4 to 0.8 mg of the lyophilized powder in 200 μ L pH 11 water, with the addition of 1 μ L of 1 M dithiothreitol (DTT) to break disulfide bonds, followed by the addition of 300 μ L of pH 7.0 PBS buffer. The obtained solution was filtered through an Amicon filter with a molecular weight cutoff of 10 kDa at 14000 rpm for 15 min to remove free DTT. The filtration was repeated 3 times. The concentration of α -Syn in the solutions was determined by spectrophotometry (Nanodrop[®] ND-1000, DE) using the molar extension coefficients 1280 $\text{cm}^{-1}\cdot\text{m}^{-1}$ and 120 $\text{cm}^{-1}\cdot\text{m}^{-1}$ for tyrosine and cysteine at 280 nm, respectively. Aliquots were stored at $-20\text{ }^{\circ}\text{C}$.

Single cysteinyl α -Syn (with a cysteine residue at the C terminus) and double cysteinyl α -Syn (with two cysteine residues at both the N and C terminus) were labeled with ultra-stable Cy3 and regular Cy3, respectively, both containing a maleimide functional group. When labeling single cysteinyl α -Syn, excess ultra-stable Cy3 was added (the ratio between ultra-stable Cy3 and α -Syn was 10:1). When labeling double cysteinyl α -Syn, the ratio between regular Cy3 and α -Syn was 1:1. α -Syn was mixed with fluorophores and subjected to intermittent gentle vortexing. The reaction was kept in the dark at room temperature. After 2 h, the mixture was added to ~300 μ L of PBS buffer and filtered through an Amicon filter (molecular weight cutoff = 10 kDa) at 14000 rpm for 15 min to remove free fluorophores. The filtration was repeated 3 times. The filtrate was discarded and the retentate was collected. The concentration of each fluorophore-labeled α -Syn was determined by spectrophotometry, using equation 1. The absorbance of the fluorophore at 280 nm was approximately 8% of that at 552 nm, and this value was subtracted when measuring protein concentration at 280 nm using the following equation:

$$C_{\alpha-syn} = \frac{[A_{280} - (0.08 \times A_{552})]}{\epsilon_{\alpha-syn}} \quad (1)$$

The labeling efficiency was calculated using the following equation:

$$labeling\ efficiency\ (\%) = \frac{\left(\frac{\epsilon_{\alpha-syn}}{\epsilon_{fluorophore}} \times A_{552} \right)}{[A_{280} - (0.08 \times A_{552})]} \times 100 \quad (2)$$

The labeling efficiency for single cysteinyl α -Syn and double cysteinyl α -Syn was 40-50% and 22-25%, respectively. Stock solutions and aliquots were stored at -20°C under inert (argon) atmosphere.

Single-molecule photobleaching

Coverslips were first functionalized with 167 μ M APS, followed by functionalization with mixed PEG (mPEG-SVA: MAL-PEG-SVA = 100:1). The double cysteinyl α -Syn with commercially available Cy 3 labeled at one end was immobilized onto the PEG-lated surface through the other end. The covalent immobilization of Cy 3 onto the PEG-lated surface ensured that fluorophores were under constant excitation and emission. Single-molecule photobleaching experiments were conducted on an Olympus IX71 instrument, with the same setup as regular experiments. The

video was recorded with ~ 30 s duration. Fluorophores from commercial sources usually bleach within this time window.

AFM imaging

APS-mica was used in AFM experiments. Mica strips (5.0×1.5 cm) were freshly cleaved and functionalized by immersion into aqueous 167 μ M APS solution for 30 min. APS-mica was then thoroughly rinsed with DI water, dried with argon flow and stored in a vacuum chamber. The APS-mica strip was cut into ~0.75×0.75 cm pieces for the sample preparation. α -Syn samples were diluted from freshly prepared stock solution to 10 nM with pH 7.0 10 mM PBS buffer. 8 μ L of diluted samples were deposited onto APS-mica surfaces for 2 min, followed by a thorough rinse with DI water. The specimens were dried with argon flow and kept in a vacuum chamber overnight. Next, the specimens were mounted onto metal discs with double-side tape.

AFM imaging was performed on a multimode 8 AFM (Bruker Nano, Santa Barbara, CA) equipped with PeakForce modules. Images were acquired in air using MSNL tips (Bruker Nano, Santa Barbara, CA) with a nominal spring constant of 0.5 N/m. AFM images were scanned with 512×512 pixels at rates of 4-6 Hz. AFM images were flattened by Nanoscope Analysis (Bruker Nano, Santa Barbara, CA). Volume analysis of fresh α -Syn samples was conducted using Femtoscan (Advanced Technologies Center, Moscow, Russia) software. “Enum features”, a functional tool provided by the software, was used to measure volumes of the protein on AFM images. The background was subtracted over the non-covered surface area. The volume values were obtained and then subjected to a Gaussian fit using Origin 6.0 software.

Supplementary results

To test the photophysical properties of ultra-stable fluorophores, fluorophores were covalently immobilized to the cover slip via SVA-PEG-SVA (SVA-PEG-SVA: mPEG = 1:100), of which one NHS group was used to link to the APS on the substrate while the other one was used for fluorophore conjugation. The data showed the majority of ultra-stable fluorophores did not bleach and blink during the data acquisition time (Supplementary movie 1). An example of a time trajectory of dye intensity is shown in Fig. S1. Overall, the fluorophores did not photobleach or photoblink within the data acquisition time.

α -Syn that contains two cysteines at the N- and C-terminus was labeled with regular Cy3

at one end, whereas the other end was used for conjugation with a Mal-PEG-SVA-functionalized cover slip. Bright spots are sparsely observed in Figure S2A, suggesting the homogeneity of surface coverage. There were no such spots on an mPEG-SVA functionalized surface, suggesting that non-specific binding of α -Syn is very low (Fig. S2B). To see if any fluorophore-labeled single cysteinyl α -Syn molecule nonspecifically adsorbed onto the surface, 1 nM of Cy3-labeled single cysteinyl α -Syn was added on a mixed PEG surface and imaged with TIRF (Fig. S3A). The number of nonspecifically adsorbed particles was then counted. The ratio of nonspecific adsorption events to specific binding events was substantially lower than 10%(3), a threshold number used for evaluating the fidelity of single-molecule detection. To examine if mPEG-SVA successfully passivated the substrate, 1 nM of fluorophore-labeled single cysteinyl α -Syn was directly deposited on an untreated glass slide and imaged with TIRF (Fig. S3B). The adsorbed particles were then spotted. A large number of fluorophores are observed because of strong nonspecific adsorption. The insets in Fig. S3A and Fig. S3B show schematics of individual experimental designs. The backgrounds of Fig. S3A and Fig. S3B are intentionally adjusted at the same level for better comparison. The latter two controls showed mPEG-SVA was suitable and capable of eliminating nonspecific adsorption. We next performed photobleaching experiments to ensure that immobilized α -Syn molecules were indeed single-molecules. A typical photobleaching trace is shown in Fig S2C. Over 95% of traces displayed single-step bleaching (Fig. S2D), suggesting that appropriate conditions for the single-molecule fluorescence experiments were identified. Only a few traces showed two-step bleaching, suggesting that colocalization of two α -Syn molecules within the excitation spot is a rare event. Third, we examined the self-assembling ability of α -Syn into aggregates. The protein stoichiometry in solution was inspected by AFM imaging (Fig. S4A). The protein appeared as small globular particles (blobs) of uniform size (Fig. S4B) corresponding to the monomeric size of the protein(4).

By optimizing the concentrations of α -Syn and the ratio between PEGs, well separated dimeric complexes of α -Syn molecules were acquired with sufficient yields at 1 nM of fluorophore-labeled α -Syn for injection, 25 pM fluorophore-free α -Syn for immobilization, and 1:100 of MAL-PEG-SVA: mPEG-SVA for surface passivation (Fig. S5). Two dimerization events from the same movie are shown in Fig. S6. Only the area of interest is shown. Spots of interest are highlighted and numbered 1 and 2. At frame A, there are fluorophores existing on

both spots, indicating the occurrence of dimerization events. At frame B, fluorophore 1 (spot 1) flies away after a short dwell, while fluorophore 2 (spot 2) stays for a longer time until frame C. Assemblies of typical fluorescence time traces of dimerization events of A30P, 4E6K and A53T are shown in Figs. S8, S9 and S10, respectively.

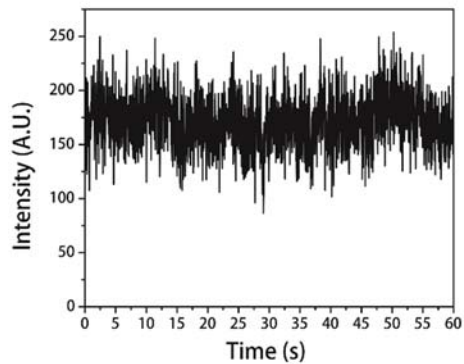


Figure S1. A time trajectory of an ultra-stable fluorophore covalently linked to the substrate via SVA-PEG-SVA.

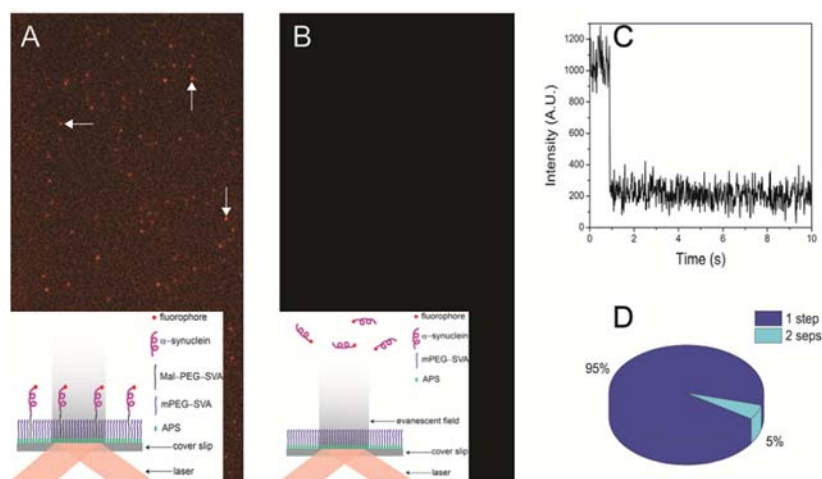


Figure S2. Selected frames of the fluorescence intensities for (A) immobilized Cy3 α -Syn and (B) control experiment involving the omission of Mal-PEG-SVA, thereby preventing covalent immobilization of Cys- α -Syn. Arrows in panel A point to selected typical dyes that continuously fluoresce until bleach. The insets in A and B show schematics for each experimental setup. (C) A single-molecule photobleaching trace shows typical one-step bleaching. (D) Pie histogram for the distribution of one-step and two-step bleaching events. The background levels in A and B were adjusted at the same values.

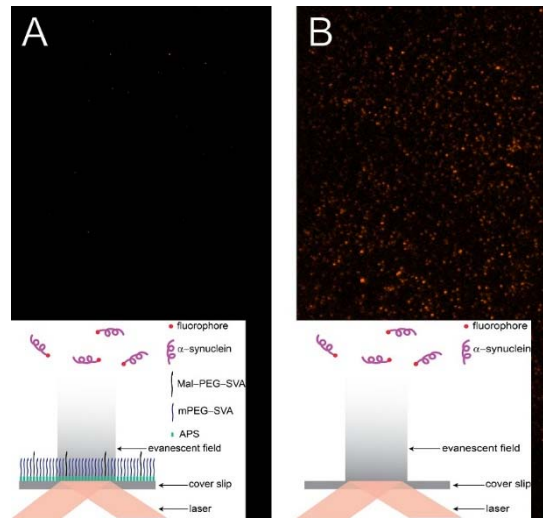


Figure S3. Comparison of 1 nM labeled α -Syn non-specific adsorption on various surfaces. (A) Non-specific adsorption on the mixed PEG-functionalized surface. (B) Adsorption of the same labeled α -Syn on a clean cover slip.

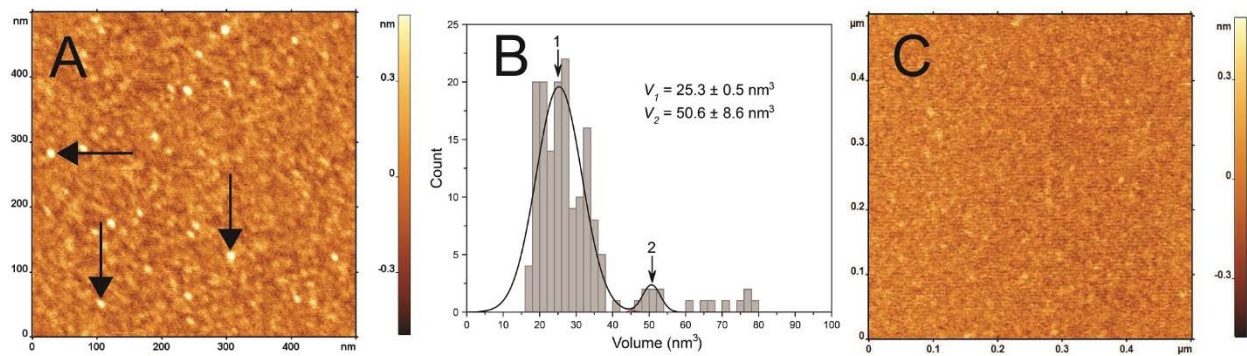


Figure S4. AFM analysis of the WT a-Syn sample. (A) AFM image ($500 \text{ nm} \times 500 \text{ nm}$) in which arrows point to spherical features corresponding to α -Syn molecules. The Z scale has a maximum of 0.5 nm. (B) Histogram showing the distribution of volumes obtained from measurements of 165 α -Syn molecules. Two peaks corresponding to monomer ($25.3 \pm 0.5 \text{ nm}^3$) and dimer ($50.6 \pm 8.6 \text{ nm}^3$) are clearly shown. Two deconvolved individual fits are well overlaid with the sum that is shown as the black solid line. The ratio between monomer and dimer is estimated to be 94:6. (C) AFM image of a sample from a control experiment in which only buffer without the protein was imaged ($500 \text{ nm} \times 500 \text{ nm}$).

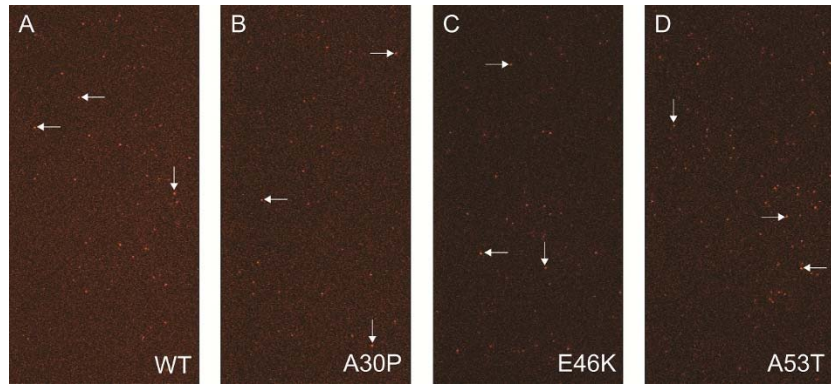


Figure S5. Snapshots of the dimerization events for WT (A), A30P (B), E46K (C) and A53T (D), respectively. Arrows indicate a few typical dimer formation events. The ratios between Mal-PEG-SVA and mPEG was 1:100.

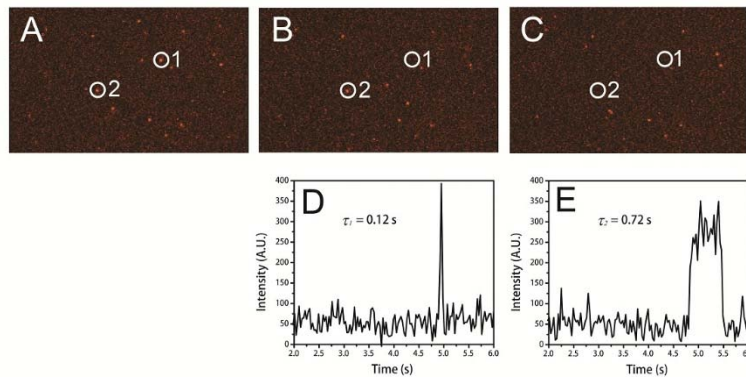


Figure S6. Three frames (A, B and C) taken from supplementary movie 1, which show two dimerization events with different lifetimes. The corresponding traces of spots 1 and 2 are shown in D and E, respectively.

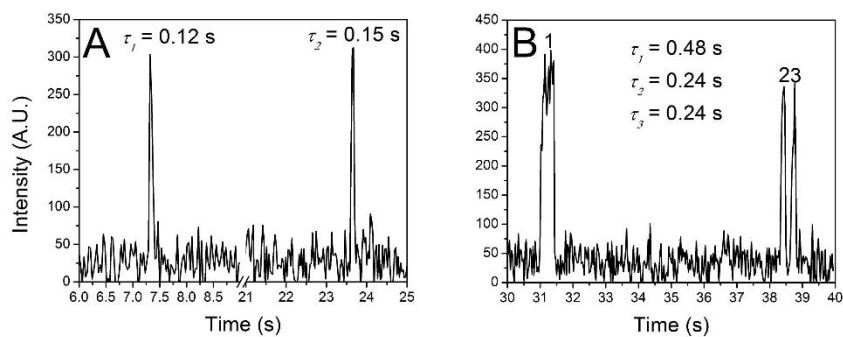


Figure S7. Multiple dissociation and rebinding events observed along the same time trajectory for WT α -Syn. (A) two dimerization events separated with a long time interval. (B) Three dimerization events observed in a time interval of less than 10 s. Event 3 appeared in less than 2 s after event 2. The lifetimes for each event are indicated.

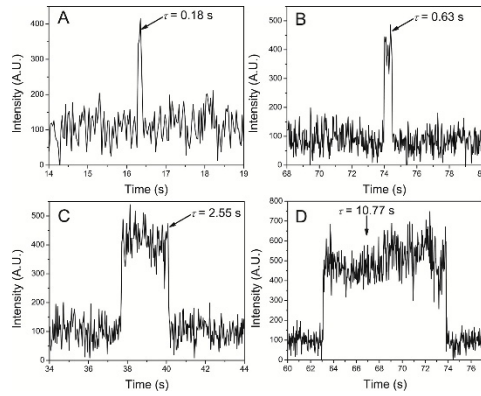


Figure S8. Typical fluorescence time traces of four events for A30P dimer. The lifetimes are indicated.

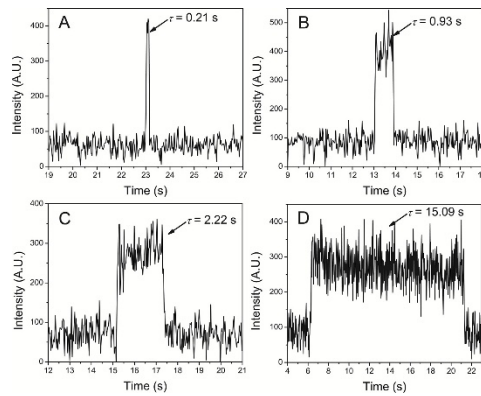


Figure S9. Typical fluorescence time traces of four events for E46K dimer. The lifetimes are indicated.

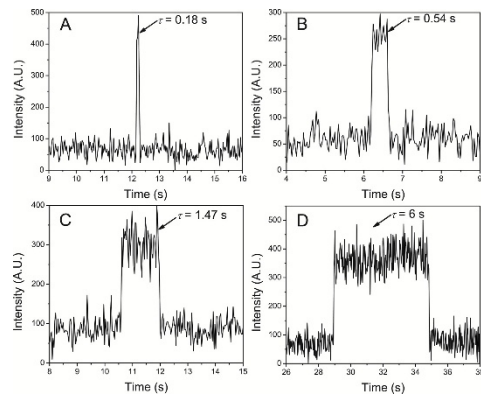


Figure S10. Typical fluorescence time traces of four events for A53T dimer. The lifetimes are indicated.

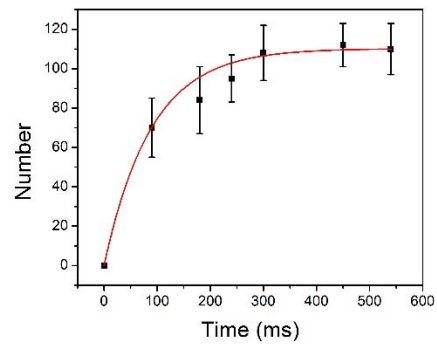


Figure S11. Time dependence of α -Syn dimerization events during the initial twenty frames. This graph shows that a plateau is reached at ~ 300 ms. Numbers are averaged over at least three consecutive frames. Error bars indicate \pm SD.

Supplementary tables

Table S1. Comparison of goodness-of-fitting (R^2) among single exponential (1-exp), double exponential (2-exp), and triple exponential (3-exp) decays for α -Syn proteins.

	R^2 (1-exp)	Lifetime (ms)	R^2 (2-exp)	Lifetime (ms)	R^2 (3-exp)	Lifetime (ms)
						$\tau_1 = 170 \pm 6$
WT	0.96	$\tau = 278 \pm 9$	0.99	$\tau_1 = 197 \pm 3$ $\tau_2 = 3334 \pm 145$	0.99	$\tau_2 = 1.7^a$ $\tau_3 = 3262 \pm 197$ $\tau_1 = 506 \pm 20$
A30P	0.95	$\tau = 1486 \pm 30$	0.99	$\tau_1 = 693 \pm 14$ $\tau_2 = 4998 \pm 134$	0.99	$\tau_2 = 2160 \pm 137$ $\tau_3 = 11328 \pm 881$
E46K	0.93	$\tau = 465 \pm 11$	0.98	$\tau_1 = 292 \pm 5$ $\tau_2 = 3593 \pm 140$	Fit does not converge ^b	NA
A53T	0.88	$\tau = 529 \pm 25$	0.99	$\tau_1 = 226 \pm 6$ $\tau_2 = 2931 \pm 104$	0.99	$\tau_1 = 226 \pm 5^c$ $\tau_2 = 2931 \pm 122^c$

Note: ^a the obtained value of fitting parameters A_2 is negative; ^b failure to perform 3-exp fit; ^c 3-exp fit gives two but not three lifetimes.

Table S2. Lifetimes of four protein dimers from individual experiments

Sample	Experiment number	τ_1 (ms, \pm fitting error)	τ_2 (ms, \pm fitting error)
WT	1	159 ± 6	$2675 \pm 1002^*$
	2	200 ± 2	$8397 \pm 392^*$
	3	244 ± 6	$2556 \pm 83^*$
A30P	1	921 ± 12	$8441 \pm 319^*$
	2	505 ± 33	$3297 \pm 153^*$
	3	660 ± 15	$6834 \pm 199^*$
E46K	1	254 ± 12	$1991 \pm 304^*$
	2	324 ± 9	$2938 \pm 145^*$
	3	299 ± 7	$5944 \pm 251^*$
A53T	1	216 ± 7	$2513 \pm 102^*$
	2	324 ± 9	$4076 \pm 85^*$
	3	202 ± 12	$2191 \pm 430^*$

Note: τ_1 and τ_2 denote the lifetimes of type 1 and type 2 dimers, respectively. *In each case, the lifetime of type 2 dimer is significantly longer than that of type 1, $p < 0.01$.

Table S3. Activation energy barriers for α -Syn dimers

	WT ($k_B T$)	A30P ($k_B T$)	E46K ($k_B T$)	A53T ($k_B T$)
Type-1	27.8 ± 0.4	29.1 ± 0.6	28.2 ± 0.5	28.0 ± 0.7
Type-2	30.7 ± 1.3	31.1 ± 0.8	30.7 ± 1.2	30.5 ± 1.1

Supplementary movies

Movie S1. Footage of stability of ultra-stable Cy3 covalently immobilized on cover slip

Movie S2. Footage of photobleaching of regular Cy3 covalently immobilized on cover slip

Movie S3. Footage of WT α -Syn dimerization.

Movie S4. Footage of A30P α -Syn dimerization.

Movie S5. Footage of E46K α -Syn dimerization.

Movie S6. Footage of A53T α -Syn dimerization.

References

1. Krasnoslobodtsev, A. V., J. Peng, J. ..., Y. L. Lyubchenko. 2012. Effect of spermidine on misfolding and interactions of alpha-synuclein. *PLoS One* 7:e38099.
2. Krasnoslobodtsev, A. V., I. L. Volkov, ..., Y. L. Lyubchenko. 2013. alpha-Synuclein Misfolding Assessed with Single Molecule AFM Force Spectroscopy: Effect of Pathogenic Mutations. *Biochemistry* 52:7377-7386.
3. Roy, R., S. Hohng, and T. Ha. 2008. A practical guide to single-molecule FRET. *Nat Methods* 5:507-516.
4. Shlyakhtenko, L. S., J. Gilmore, ..., Y. L. Lyubchenko. 2009. Molecular mechanism underlying RAG1/RAG2 synaptic complex formation. *J. Biol. Chem.* 284:20956-20965.